Beam combining of quantum cascade laser arrays

Benjamin G. Lee,[1] Jan Kansky,[2] Anish K. Goyal,[2] Christian Pflügl,[1] Laurent Diehl,[1] Mikhail A. Belkin,[1] Antonio Sanchez,[2] Federico Capasso[1*]

[1]*Harvard University, School of Engineering and Applied Sciences, Cambridge, MA, USA*
[2]*MIT Lincoln Laboratory, Lexington, MA, USA*
capasso@seas.harvard.edu

Abstract: Wavelength beam combining was used to co-propagate beams from 28 elements in an array of distributed-feedback quantum cascade lasers (DFB-QCLs). The beam-quality product of the array, defined as the product of near-field spot size and far-field divergence for the entire array, was improved by a factor of 21 by using wavelength beam combining. To demonstrate the applicability of wavelength beam combined DFB-QCL arrays for remote sensing, we obtained the absorption spectrum of isopropanol at a distance of 6 m from the laser array.

OCIS codes: (140.5965) Semiconductor lasers, quantum cascade; (140.3298) Laser beam combining; (140.3490) Lasers, distributed-feedback; (140.3290) Laser arrays

References and links

1. F. Capasso, C. Gmachl, D. L. Sivco, and A. Y. Cho, "Quantum cascade lasers," Phys. Today **55**, 34 (2002).
2. A. Kosterev and F. Tittel, "Chemical sensors based on quantum cascade lasers," IEEE J. Quantum Electron. **38**, 582 (2002).
3. Y. Bai, S. R. Darvish, S. Slivken, W. Zhang, A. Evans, J. Nguyen, and M. Razeghi, "Room temperature continuous wave operation of quantum cascade lasers with watt-level optical power," Appl. Phys. Lett. **92**: 101105 (2008).
4. A. Lyakh, C. Pflugl, L. Diehl, Q. J. Wang, Federico Capasso, X. J. Wang, J. Y. Fan, T. Tanbun-Ek, R. Maulini, A. Tsekoun, R. Go, and C. Kumar N. Patel, "1.6 W high wall plug efficiency, continuous-wave room temperature quantum cascade laser emitting at 4.6 μm," Appl. Phys. Lett. **92**, 111110 (2008).
5. R. Maulini, A. Mohan, M. Giovannini, J. Faist, and E. Gini, "External cavity quantum-cascade lasers tunable from 8.2 to 10.4 μm using a gain element with a heterogeneous cascade," Appl. Phys. Lett. **88**, 201113 (2006).
6. B. G. Lee, M. A. Belkin, R. Audet, J. MacArthur, L. Diehl, C. Pflugl, D. Oakley, D. Chapman, A. Napoleone, D. Bour, S. Corzine, G. Hofler, J. Faist, and F. Capasso, "Widely tunable single-mode quantum cascade laser source for mid-infrared spectroscopy," Appl. Phys. Lett. **91**, 231101 (2007).
7. B. G. Lee, M. Belkin, C. Pflugl, L. Diehl, H. A. Zhang, R. M. Audet, J. MacArthur, D. Bour, S. Corzine, G. Hofler, and F. Capasso, "Distributed feedback quantum cascade laser arrays," IEEE J. Quantum Electron. **45**, 554–565 (2009).
8. T. Y. Fan, "Laser Beam Combining for High-Power, High-Radiance Sources," IEEE J. Sel. Top. Quantum. Electron. **11**, 567 (2005).
9. V. Daneu, A. Sanchez, T. Y. Fan, H. K. Choi, G. W. Turner, and C. C. Cook, "Spectral beam combining of a broad-stripe diode laser array in an external cavity," Opt. Lett. **25**, 405–407 (2000).
10. R. K. Huang, B. Chann, L. J. Missaggia, J. P. Donnelly, C. T. Harris, G. W. Turner, A. K. Goyal, T. Y. Fan, and A. Sanchez-Rubio, "High-brightness wavelength beam combined semiconductor laser diode arrays," IEEE Photon. Tech. Lett. **19**, 209–211 (2007).
11. S. J. Augst, A. K. Goyal, R. L. Aggarwal, T. Y. Fan, and A. Sanchez., "Wavelength beam combining of ytterbium fiber lasers," Opt. Lett. **28**, 331–333 (2003).
12. B. Chann, A. K. Goyal, T. Y. Fan, A. Sanchez-Rubio, B. L. Volodin, and V. S. Ban, "Efficient, high-brightness wavelength-beam-combined commercial off-the-shelf diode stacks achieved by use of a wavelength-chirped volume Bragg grating," Opt. Lett. **31**, 1253–1255 (2006).

#108905 - $15.00 USD Received 26 Mar 2009; revised 31 May 2009; accepted 7 Jun 2009; published 27 Aug 2009

13. R. Maulini, M. Beck, J. Faist, and E. Gini, "Broadband tuning of external cavity bound-to-continuum quantum-cascade lasers," Appl. Phys. Lett. **84**, 1659 (2004).
14. Daylight Solutions, www.daylightsolutions.com.

1. Introduction

Quantum cascade lasers (QCLs) are semiconductor lasers that emit in the mid-infrared from 3 to 24 μm [1], including the "fingerprint" region of molecular absorption. This makes QCLs particularly interesting for spectroscopic applications [2], including pollution monitoring, breath analysis, industrial process control, and remote detection of toxic chemicals and explosives. QCLs can achieve watt-level output power in continuous-wave operation at room temperature [3, 4] and can be designed to emit over a spectral range of $\sim$ 300 cm^{-1}, enabling wide wavelength tunability [5].

Arrays of distributed-feedback quantum cascade lasers (DFB-QCLs) can be made as single-mode sources covering a wide range of mid-infrared frequencies [6, 7] with potential applications in spectroscopy. For a number of applications envisioned for QCL arrays, it is important to have the beams from the individual lasers in the array propagate collinearly so that the beams overlap in the far-field. For example, for remote-sensing applications, if the beams can be collimated and propagated a long distance where they all overlap, then only a single detector is required at the end of the beam path to measure the resulting signal. However, when using a lens of focal length f to collimate the emission from the lasers in the array, each laser will point at a different angle given by $\Delta\theta = tan^{-1}(\Delta x/f)$ where $\Delta\theta$ is measured with respect to the axis of the lens and Δx is the transverse position of each laser relative to the focal point of the lens. In this case, each of the laser beams will be spatially separated in the far-field.

In this paper, we use wavelength beam combining (WBC) to overlap the beams from an array of DFB-QCL lasers in the far-field. To our knowledge, this is the first demonstration of WBC using an array of DFB lasers. We then perform absorption spectroscopy at a range of 6 m from the laser source to demonstrate a proof-of-principle application to remote sensing.

2. Wavelength beam combining

The general principle of wavelength beam combining is to take spatially separated beams with distinct optical spectra, and combine them using a wavelength-sensitive beam combiner [8]. Examples of wavelength-sensitive beam combiners are prisms and diffraction gratings, which can deflect incident beams according to their wavelength so that they propagate in the same direction after the combiner. WBC can be considered the reverse of a grating spectrometer in which a single beam of white light, containing many wavelengths, is split into angularly resolved monochromatic beams.

Wavelength beam combining of laser sources has been demonstrated for diode laser arrays [9, 10] and fiber lasers [11]. In one form of WBC, the laser array elements are incorporated in an external cavity containing a diffraction grating and transform lens. An output coupler in the cavity provides optical feedback to each of the laser elements to select their emission wavelengths and automatically causes all of the laser beams to propagate collinearly as in the experiment of [9]. This form of WBC is termed "closed-loop."

In another form of WBC, the laser array elements have their emission wavelengths selected independent of the grating that combines the beams. For example, a volume Bragg grating [12] or distributed feedback grating in the laser can be used for wavelength selection. Beam combining is then achieved through the use of a diffraction grating in combination with a transform lens, but without the need for an output coupler. This second form of WBC, termed "open-loop," is used for the work presented here.

#108905 - $15.00 USD Received 26 Mar 2009; revised 31 May 2009; accepted 7 Jun 2009; published 27 Aug 2009

3. DFB-QCL array

We present an array of distributed-feedback quantum cascade lasers (DFB-QCLs) where we use wavelength beam combining to co-propagate the beams, as shown in Fig. 1.

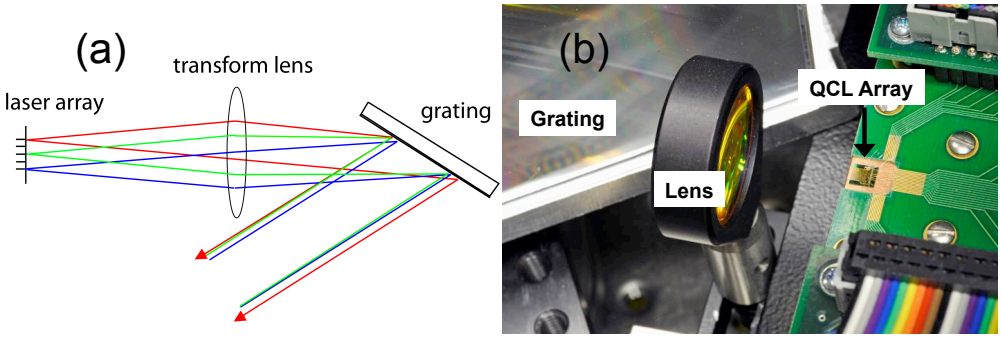

Fig. 1. (a) Schematic diagram of wavelength beam combining with an array of distributed-feedback quantum cascade lasers (DFB-QCLs). The emission wavelengths of the lasers are selected by the individual DFBs on each laser ridge in the array. Beam combining is accomplished by a suitably placed grating and transform lens that overlap the beams from each laser in both the near-field and far-field. (b) Photograph of the actual wavelength beam combining setup with the DFB-QCL array.

Our DFB-QCL array is composed of 32 single-mode ridge lasers emitting at frequencies from 1061 to 1148 cm^{-1} with the emission frequency of adjacent lasers separated by $\sim$ 2.74 cm^{-1}. The laser ridges are each 15-μm wide and separated by a center-to-center distance of 75 μm. The QCL active region for this array is a bound-to-continuum design for emission around 9-μm wavelength, as reported in [13], and the fabrication and performance of the array is detailed in [6]. The polarization of the optical output is perpendicular to the array dimension as is usual for QCLs. The DFB-QCL array was connected to a custom-built electronics controller, which allows us to individually address and power each of the laser devices in the array. Out of the 32 laser ridges, only 28 were operational, with lasers #1, 21, 22 and 32 not emitting. The DFB-QCL array is oriented so that the plane of the lasers is horizontal and parallel to the plane of the optical table. This array was not fabricated in a way to allow CW operation. The array was operated pulsed with 50-ns-long pulses at a repetition rate of 20 kHz. The maximum output power for individual lasers in the array ranged from 20 to 250 mW; the causes of this large variability are discussed in depth in [7].

A 2.5-cm-diameter ZnSe lens (f = 2.5 cm) was placed one focal distance away from the front facets of the DFB-QCL array. The lens acts to transform the position of the laser element in the array into an angle of incidence on the grating. The lens position was adjusted to ensure that the individual laser beams were collimated and that beams near the center of the array propagate on-axis; this was verified using a thermal IR camera to image the beam spots.

An aluminum-coated reflection grating with 750 lines/cm (blaze wavelength = 12 μm) was inserted in the beam path after the transform lens at a distance of about 3 cm away from the lens. The grating is attached to a rotation stage, allowing it to be rotated in a plane parallel to the laser array. The grating is approximately located one focal distance away from the lens so that the beams overlap at the grating. However, the size of the components and the need to ensure that the beam path remain unobstructed constrained the placement of the grating. The required angle for the grating to co-propagate all the beams can be deduced from the grating equation:

#108905 - $15.00 USD Received 26 Mar 2009; revised 31 May 2009; accepted 7 Jun 2009; published 27 Aug 2009

$$d(sin\theta_m + sin\theta_n) = m\lambda_n. \quad (1)$$

Here d is the groove spacing of the grating, θ_m is the output angle of the m-th diffraction order, θ_n is the incident angle of the n-th laser beam on the grating, and λ_n is the wavelength of that laser. We have $m = 1$, as our grating is blazed for high efficiency in first diffraction order. The incident angles θ_n of the lasers in the array are all different, with $\theta_n = \theta_{grating} + tan^{-1}(x_n/f)$, where x_n is the position of the n-th laser in the array and f is the focal length of the transform lens. For all the beams to co-propagate, we require that all the lasers in the array have the same output angle θ_m from the grating. From equation 1 we see that this entails that the angle of the grating $\theta_{grating}$ should be $\sim$ 55 degrees. We set the grating at this angle and then made fine adjustments until the beams from the extreme ends of the array (lasers 2 and 31, since 1 and 32 were not working) were overlapped.

4. Near and far-field beam profiles

We used a thermal IR camera to get images of the beams coming off the grating. A flat mirror was placed in the beam path, just after the grating, to direct the beams to a convenient location for measurements. We placed the IR camera in the path of the laser beams, and imaged the mirror surface to view the beam profile at that location which was taken to be the near-field of the system. A representative near-field image of one of the laser beams is shown in Fig. 2(a). The beam is clipped by the edges of the ZnSe transform lens, which is 2.5 cm in diameter. This occurs because of the large beam divergence of the light emitted from each QCL — not all of the light can be collected by the lens. The circular beam transmitted through the lens becomes elliptical after the grating because of geometric magnification due to diffraction; the major axis is $\sim$ 3.5 cm and the minor axis is still 2.5 cm.

The horizontal fringes in the near-field are due to interference between the direct emission from the laser facet and light which is reflected from the laser submount. A portion of the emitted laser beam intercepts the submount because the chip is slightly recessed from the edge of the submount. The fringe spacing is consistent with the $\sim 200-\mu$m thickness of the laser-chip substrate.

In order to image the far-field beam profiles, we placed a spherical mirror with radius of curvature equal to 2.88 m in the path of the beams. The spherical mirror was angled slightly so that the reflected beam could be focused onto the imaging plane of the IR camera (the camera's lens was removed) which was placed in the focal plane (f = 1.44 m) of the mirror. By individually imaging all of the beams from the laser array, we can determine the spot size of the beams (in angular units) and we can also quantify the relative pointing between the beams in the far-field.

The far-field beam profile of a representative laser is shown in Fig. 2(b), and has an Airy ring pattern. Taking a linescan of the far-field beam profile (Fig. 2(c)), we can quantify the angular extent of the main lobe of the Airy pattern, from null to null, as 0.93 milliradians in the horizontal direction and 1.3 milliradians in the vertical direction. For comparison, the diffraction-limited spot size at 9-μm wavelength for a beam collimated with a 2.5-cm-diameter lens is $\theta \sim 2.44\lambda/D$ and is calculated to be 0.86 milliradians. The beam divergence of an individual laser is therefore $\sim 1.5\times$ the diffraction-limit in both dimensions. Although we do not know why the beam quality is not closer to the diffraction-limit, it is not due to finite spectral width of the QCLs of $<$0.1 cm^{-1} which would result in a smearing of the far-field in the beam-combining dimension of $<$0.06 mrad.

#108905 - $15.00 USD Received 26 Mar 2009; revised 31 May 2009; accepted 7 Jun 2009; published 27 Aug 2009

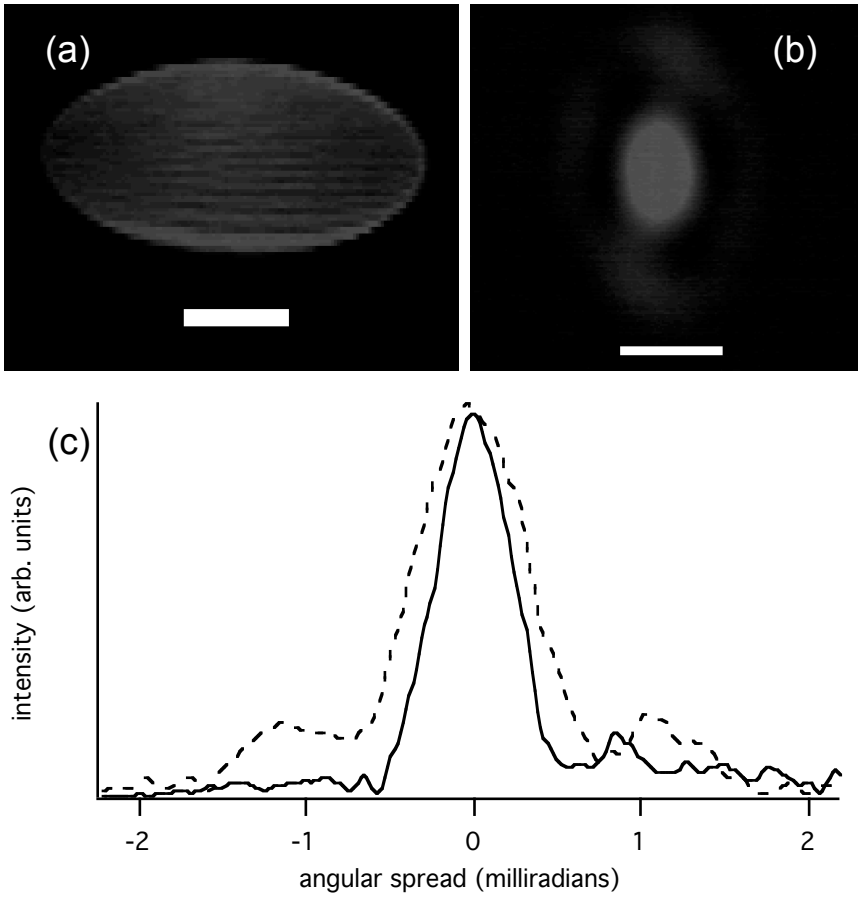

Fig. 2. (a) Image of the beam of a representative laser, just after it has been reflected from the grating. The white bar is 1 cm. (b) Image of the far-field spot of a representative laser. The white bar is 1 milliradian. (c) Linescan in the horizontal (solid) and vertical (dotted line) directions of the far-field image of a representative laser.

5. Beam overlap

The overlap of the beams in the far-field can be determined by individually imaging all the beams and overlaying those images to measure any shifts in beam pointing. Fig. 3(a) shows a composite image of the beam spots from 4 different laser elements in the array (#18, 24, 28, 31). All of the beams lie on a horizontal line. The center-to-center distance between the beam spots corresponds to a difference in beam pointing. Lasers 18 and 31 have the largest difference in beam pointing for any two lasers in the array — 2 milliradians.

Fig. 3(b) plots the pointing of laser beams from the entire array. The pointing error is measured along the beam-combining dimension relative to laser 31. The Fig. compares the experimental results to a calculation of the pointing error using the grating equation (Eq. 1) where we input the wavelengths of the DFB-QCL array and a grating angle of 54.65 degrees. There is good agreement between the results and the calculation. The residual pointing error is due to the fact that the grating's angular dispersion is not a linear function of frequency while the laser frequency varies linearly with position in the array.

We achieved beam combining with a residual pointing error of 2 milliradians in the worst

#108905 - $15.00 USD Received 26 Mar 2009; revised 31 May 2009; accepted 7 Jun 2009; published 27 Aug 2009

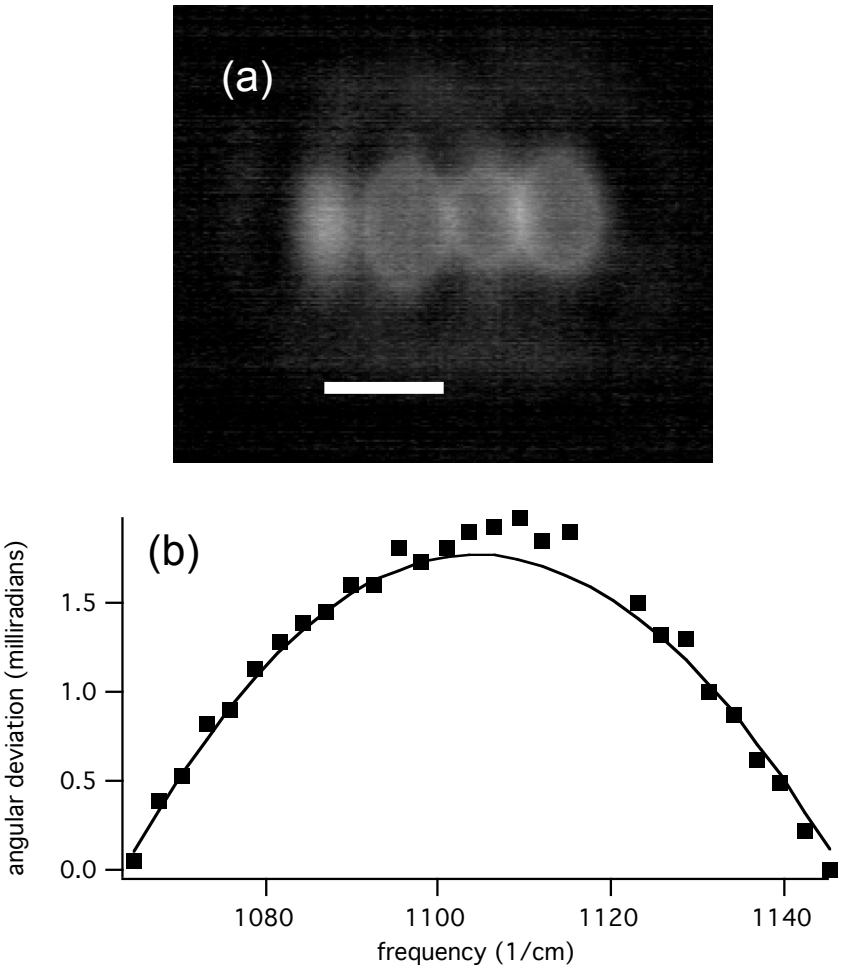

Fig. 3. (a) Image of several lasers showing the extent of the residual pointing error of the beams. From the left, we have laser elements #18, 24, 28, and 31 in the array. Lasers 18 and 31 have the largest relative pointing error in the entire array. The white bar is 1 milliradian. (b) A plot of the angular deviation of the laser beams, as a function of the laser frequency. Squares represent the pointing of laser beams from the entire array as measured relative to the pointing of laser 31 (rightmost point in the plot). The line is a calculation of the beam pointing using the grating equation (Eq. 1) given the wavelengths of the DFB-QCL array and a grating angle of 54.65 degrees.

#108905 - $15.00 USD Received 26 Mar 2009; revised 31 May 2009; accepted 7 Jun 2009; published 27 Aug 2009

case for the beams. Defining the beam-quality product of the array as the product of the near-field beam size and the far-field divergence, we calculate a beam-quality product of (3.5 cm)(2 mrad + 0.93 mrad) = 103 mm·mrad for the beam-combined system. For reference, using our null-to-null definition of far-field divergence, a diffraction-limited beam has a beam-quality product of 22 mm·mrad. Without WBC, the beam-quality product would be (2.5 cm)(86 mrad + 0.93 mrad) = 2173 mm·mrad, or a factor of 21 higher. The improvement in beam-quality product that is achievable by WBC is dependent upon the fill-factor of the array. In the limiting case of near-unity fill-factor, which can be achieved by using a spherical microlens array to increases the effective mode size for each laser in the array by 5x, it is calculated that WBC improves the beam quality by a factor of $\sim$12.

In order to reduce the residual pointing error even further, we could use a laser array where either the spacing of frequencies in the array or the physical spacing of the laser elements is not linear. In particular, the required spacing of the laser frequencies or laser element positions can be calculated using Eq. 1. Alternatively, it may be possible to reduce the pointing error through the choice of diffraction grating and transform lens.

We can also steer the laser beams by temperature-tuning to change the lasers' emission frequencies. The change in frequency results in a shift in the diffracted angle of the laser beam. We measured the temperature-tuning of the lasers to be -0.073 cm^{-1}/K. We used a thermoelectric (Peltier) device to heat/cool the laser submount, varying the temperature from 293 to 332 K. For one selected laser, this temperature change corresponded to a frequency change from 1112.3 to 1109.5 cm^{-1}, resulting in an angular shift of the beam of 1.8 milliradians. The calculated angular shift using Eq. (1) is 1.7 milliradians.

The grating efficiency, defined as the ratio of the power in the first-order diffracted beam to the incident laser power, was measured to be 55%. For the weakest laser in our array with 20 mW output power, this translates to 11 mW coupled to the far-field beam neglecting atmospheric absorption; for stronger lasers in the array the power coupled to the far-field ranges up to 140 mW. Based on the efficiency curves of commercially available blazed gratings, it should be possible to achieve >90% diffraction efficiency with the proper choice of grating and polarization of the incident beams. Typically, blazed gratings are more efficient for p-polarized light (electric-field perpendicular to the grating grooves), whereas QCLs are TM polarized (s-polarized at the grating in a WBC configuration). Therefore, it may be necessary to use a half-wave plate to access the highest possible diffraction efficiency.

6. Remote-sensing demonstration

To demonstrate the potential of WBC DFB-QCL arrays for remote sensing, we performed a simple absorption-spectroscopy measurement at a distance of 6 m from the laser array. At a distance of 6 m, a BaF_2 lens (f = 19 cm and diameter = 5 cm) was placed in front of a thermoelectrically-cooled Vigo MCT detector (model PCI-3TE-12 1x1) to collect the laser light from the array onto the detector. A BaF_2 fluid cell (chamber thickness 27.2 μm) was placed in the path of the beams between the lens and the detector. The fluid cell was filled with isopropanol for sample measurements or left empty to measure the background.

To measure the spectrum, the lasers were fired sequentially, and the intensities of the transmitted beams were recovered from the detector using a gated integrator. After taking the background and sample spectra, we obtained the absorption spectrum using a frequency table with data for each laser in the array (Fig. 4). The spectra took less than 10 s to obtain using the DFB-QCL array. The present limitations on speed are due to the noise in the measurement system which requires the averaging of many laser pulses, the fastest repetition rate (100 kHz) achievable using custom-built electronics, and the delay in transmitting both control instructions and data over a slow serial connection between the electronics and our lab computer. The

#108905 - $15.00 USD Received 26 Mar 2009; revised 31 May 2009; accepted 7 Jun 2009; published 27 Aug 2009

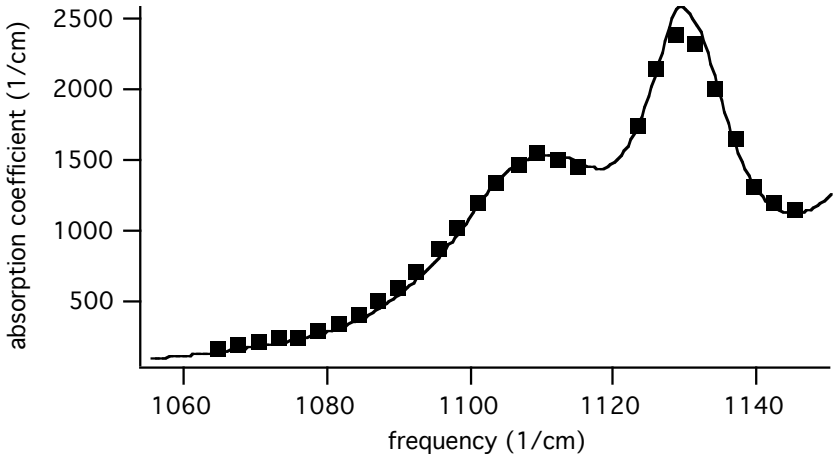

Fig. 4. Absorption spectrum of isopropanol measured using the WBC DFB-QCL array at a distance of 6 m (squares). Fourier-transform infrared-spectrometer measurement of the same sample using a Bruker Vertex 80v FTIR instrument (solid line).

noise in the measurement is dominated by electromagnetic pickup in our custom-built electronics rather than by any fundamental sources of noise in the lasers or the amount of laser signal available. With lower-noise detection electronics and a higher data-rate connection, the measurement time could be reduced to milliseconds or less. This is much faster than is currently possible with single-element external-cavity QCLs which typically require $\sim$1 second to scan over the full wavelength range [14].

Our results compare favorably with spectra obtained using a conventional Fourier-transform infrared (FTIR) spectrometer, which are also shown in Fig. 4. Without WBC this demonstration would not be possible with the QCL array since the laser beams would be separated by as much as 0.5 meters at a range of 6 meters.

In summary, we achieved wavelength beam combining for 28 elements of a DFB-QCL array, improving the beam-quality product by a factor of 21 as compared to without beam-combining. The efficiency of transferring the optical power to the far-field was 55%, giving far-field intensities of lasers in the array ranging from 11 to 140 mW peak power. While we have used only a small array of lasers for our demonstration, the WBC approach can be scaled to hundreds of lasers, limited only by the spacing of the individual lasers in the array and the array's total width. With laser ridge-to-ridge spacing of $\sim$10 microns and total array size of $\sim$1 cm, with a suitable transform lens to collect the light from the entire width of the array, we can potentially beam-combine up to a thousand elements.

In the future, we envision using WBC QCL arrays for remote sensing at distances of kilometers. To do so, we plan to achieve more complete overlap of the beams in the far-field, through a combination of the optical design and choosing appropriate laser frequencies, so that we eliminate the residual pointing error observed in this paper. Also, we are also currently investigating the "closed-loop" approach to WBC as it may have benefits in terms of beam overlap and simplified device fabrication. Finally, we hope to make laser arrays with higher power output, for instance watt-level peak power from each laser in the array.

#108905 - $15.00 USD Received 26 Mar 2009; revised 31 May 2009; accepted 7 Jun 2009; published 27 Aug 2009

Acknowledgments

This work was sponsored by the Department of the United States Air Force under Air Force Contract No. FA872-05-C-0002 and by the DARPA Optofluidics Center under grant number HR00-04-1-0032. The opinions, interpretations, conclusions and recommendations are those of the authors and are not necessarily endorsed by the United States Government. The authors gratefully acknowledge David Bour, Scott Corzine, and Gloria Höfler, all formerly of Agilent Laboratories, Palo Alto CA 94304 USA, for wafer growth. This work was performed in part at the Center for Nanoscale Systems (CNS) at Harvard University. Harvard-CNS is a member of the National Nanotechnology Infrastructure Network (NNIN).

#108905 - $15.00 USD Received 26 Mar 2009; revised 31 May 2009; accepted 7 Jun 2009; published 27 Aug 2009